Parametric study of the force acting on a target during an aircraft impact

Lili Eszter Laczák[*] and György Károlyi[**]
[*]*Department of Structural Engineering, Budapest University of Technology and Economics, Budapest, Hungary*
[**]*Institute of Nuclear Technics, Budapest University of Technology and Economics, Budapest, Hungary*

Summary. Analysing the consequences of potential aircraft impact into engineering structures is an issue of high importance especially in case of structures with special functions. In case of stiff structures, the global effects of an aircraft impact can be characterised by a time dependent load (reaction force) acting on the target structure. In our paper, reaction forces of different missiles (from homogenous cylinders to complex aircraft models) are calculated by the commonly applied analytic Riera model and by finite element simulations. Effect of different parameters, geometry and structural parts of aircraft (nose, tail, wings, engines) on the reaction force and the difference between the results of different models are examined and the results are evaluated.

Introduction

Analysing the effects of an aircraft impact on the global structural behaviour of a structure can be an issue of high importance in case of special target structures (e.g nuclear power plants (NPPs)). If the target structure is relatively rigid and the missile is soft (this assumption is generally valid for aircraft fuselage impacts into NPPs) then the impact can be characterised by the force acting on the target structure. If this (reaction) force is determined, then it can be applied as a time dependent load on different (typically finite element) models of the target structure. This analysis method, called force time-history analysis is included in different standards and guidelines [1-3]. In our analysis, the force acting on a rigid structure during a soft aircraft impact is calculated by the analytic Riera model [4] that is widely used in nuclear industry, and by finite element models. The effect of realistic aircraft profiles is examined, therefore, results of uniform aircraft fuselages (cylindrical missiles), aircraft fuselages with nose and tail segments, and realistic aircrafts also with wings and engines are compared.

The Riera model

The most commonly suggested method in nuclear industry to determine the reaction force acting on the target is the Riera method [4], in which the missile is assumed to be rigid-perfectly plastic and the target structure is rigid (see Fig. 1).

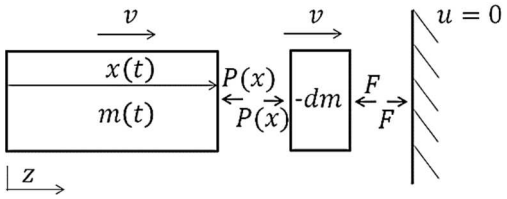

Fig. 1: Riera model of a soft missile impact into rigid target

In the model, the missile consists of two parts: an uncrushed part of length $x(t)$ and of mass $m(t)$, and an infinitesimally small part of mass $(-dm) > 0$ that crushes in the next time instant. At time t, crushing force $P(x)$ acts on the intact part of length $x=x(t)$ of the aircraft and breaks mass $(-dm)$ off the aircraft. We can write down the balance of momentum of the intact part right before and after the break off. Force $P(x)$ and reaction force $F(t)$ act on mass $(-dm)$ that slows from velocity $v(t)$ to zero during time dt, thus the balance of momentum can also be expressed. From these two equations, if the linear mass distribution $\mu(x)$ and the crushing force $P(x)$ of the aircraft are known, then the reaction force $F(t)$ can be expressed as [4-6]:

$$F(t) = P\big(x(t)\big) + \mu\big(x(t)\big) \cdot \left(\frac{dx}{dt}\right)^2. \tag{1}$$

The Riera model is widely applied, but there is a lack of detailed parametric tests on its applicability. In our previous papers [5-6], uniform aircraft fuselages (cylindrical missiles with $P(x)$=const.=P_0 and $\mu(x)$=const.=μ_0) were examined, and results of the Riera and an explicit finite element (FE) model were compared. In some ranges of parameters, we found that the results obtained from the models show significant differences because of the intense deceleration of the missile in the Riera model that did not occur in the FE model. We also found that the course of the impact mainly depends on one parameter, the damage potential, defined as the ratio of the initial kinetic energy of the missile to the work required to crush it [5-6]:

$$D = \frac{\frac{1}{2} m_0 V^2}{L P_0}, \tag{2}$$

where V is the initial velocity of the impacting missile, m_0 and L are its total mass and length, respectively, and P_0 is the characteristic value of the crushing force of the missile.

Effects of realistic aircraft profile

The central part of an aircraft fuselage can be modelled by a uniform missile, but tail and nose parts are typically lighter and softer ($\mu(x)$ and $P(x)$ are smaller). Moreover, wings and engines also have significant effects on the mass and crushing force distribution, consequently on the reaction force. To clearly see the effect of geometry and different parameters, more realistic aircraft profiles are examined in two steps. First the uniform aircraft fuselage is extended by nose and tail, then by wings and engines (see Fig. 2).

The length of the nose and the tail are 4.5 m and 4 m, respectively, while the total length of the fuselage is 17.5 m, the mean diameter of the fuselage at the central part is 2 m, the wall thickness is 0.025 m. The FE model is built in ANSYS Workbench Explicit Dynamics environment, the missile is meshed by hexahedral 8 node linear volume elements.

For the missile, we assume a quasi rigid– perfectly plastic material with strength f_y (that also includes the effect of local buckling), ultimate strain ε_u=1**,** Poisson's ratio ν=0.3 and density ρ. If ultimate strain ε_u is reached in a finite element during the impact, then it is deleted from the model. Mass per unit length μ and total mass m_0 of the missile can be directly calculated from the geometry and density of the missile. However, the definition of the crushing force $P(x)$ is not obvious, because it also includes local buckling, in our calculations we use Af_y, where A is the cross-sectional area of the cross-section adjacent to the target. Effect of FE mesh was tested and 0.16 m average FE size along the length of the missile was found to give satisfactory results.

Table 1 shows the properties of the examined fuselage cases with nose and tail. Ratio of the density and strength of the nose and tail (ρ_n, f_{ny}) to those of the central segment (ρ, f_y) are altered. In cases BN1, EN1 only the cross-section changes along the length, in cases BN2, EN2 f_y is reduced to 25%, in cases BN3, EN3 ρ_n is reduced to 25%, while in cases BN4, EN4 ρ_n and f_n are both reduced to 25% of the corresponding values at the central segment of the fuselage. Initial velocity of the missile is V=150 m/s in each case. Total mass m_0, maximum and average value of crushing force P_{max} and P_{av}, and damage potential D calculated by P_{av} as characteristic value P_0 of the crushing force are also included in the table. Figure 3 shows the shape function of mass distribution ($\mu(x)/\mu_{max}$, where μ_{max} is the maximum mass per unit length of the fuselage) and crushing force ($P(x)/P_{max}$) of cases BN1-4, EN1-4 and uniform fuselages (cylindrical missiles).

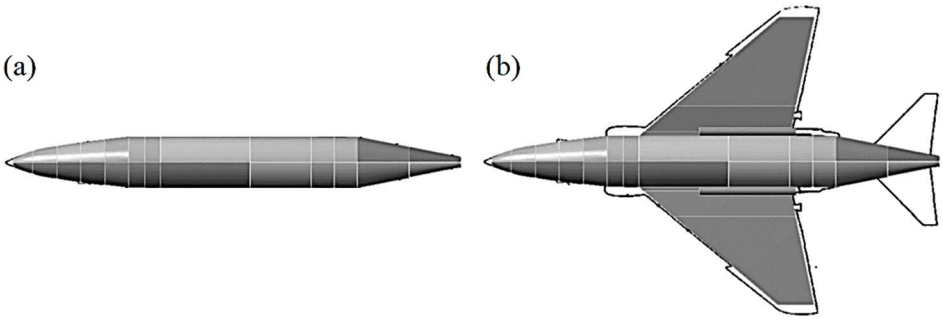

Fig. 2: Geometry of (a) aircraft fuselage with nose and tail (cases BN1-4; EN1-4); (b) simplified aircraft with wings and engines (cases BT, ET) together with geometry of a Phantom F4 fighter [7]

Table 1: Input data of cases BN1-4 and EN1-4:

case	*body*		*nose, tail*		m_0	P_{max}	P_{av}	D (P_{av})
	ρ (kg/m^3)	f_y (10^6 Pa)	ρ_n/ρ	f_{ny}/f_y	(10^3 kg)	(10^6 N)	(10^6 N)	
BN1	8000	5	1.00	1.00	17.82	0.78	0.64	18.00
BN2			1.00	0.25	17.82	0.78	0.52	22.16
BN3			0.25	1.00	14.49	0.78	0.64	14.64
BN4			0.25	0.25	14.49	0.78	0.52	18.00
EN1	8000	40	1.00	1.00	17.82	6.2	5.09	2.25
EN2			1.00	0.25	17.82	6.2	4.14	2.77
EN3			0.25	1.00	14.49	6.2	5.09	1.83
EN4			0.25	0.25	14.49	6.2	4.14	2.25

In the following diagrams, dimensionless force-time functions of different cases are represented. The dimensionless time $\tilde{t}$ and dimensionless reaction force f are calculated as:

$$\tilde{t} = t\sqrt{\frac{P_{max}}{Lm_0}},\ \ f = F/P_{max} \tag{3}$$

In the Riera approach, in case of a perfectly rigid target, the course of the impact $x(t)$ can be obtained by solving a second order differential equation [4-5], and then $f(\tilde{t})$ is obtained from the dimensionless form of Eq. (1). In the FE model, the reaction force f is also calculated from Eq. (1), where the velocity of crushing is defined as the average velocity of the intact part of the missile.

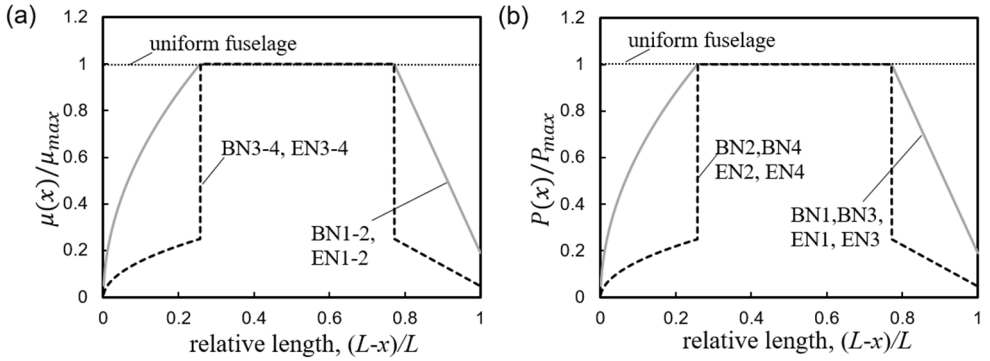

Fig. 3: Shape function of (a) mass distribution; (b) crushing force of cases BN1-BN4, EN1-EN4 and uniform fuselages

Figures 4(a) and (b) represent dimensionless reaction force—time $f(\tilde{t})$ functions of cases BN1-4 together with cylindrical missiles with the same properties in the central segment of the fuselage. We can see that the Riera and the FE model results are close to each other, deceleration of the missile is negligible in both cases. It is visible that the effect of reduced strength is much smaller than the effect of reduced density: results of cases BN1 and BN2 are close to each other, while results of cases BN1 and BN3 are significantly different. In cases BN1-4, the effect of the crushing force is negligible: in the dimensionless form of Eq. (1), the maximum relative value of $P(x)$ is 1, while the maximum value of f is 36. Consequently, the behaviour of the missile is close to the behaviour of a fluid rod, which has no strength, only mass and velocity.

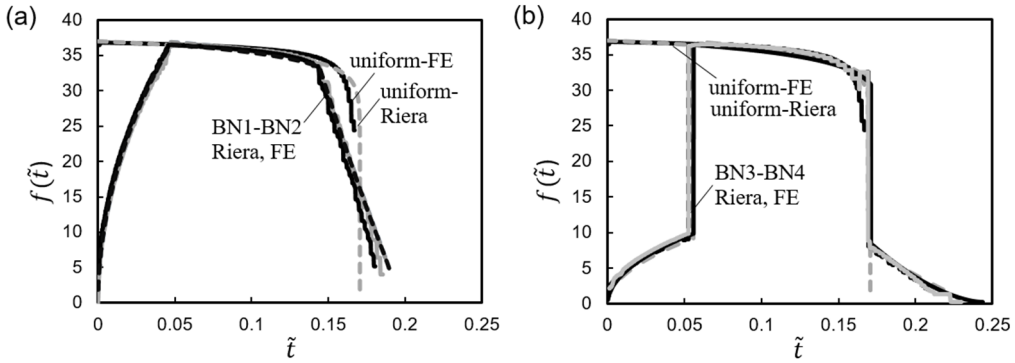

Fig. 4: Dimensionless reaction force functions $f(\tilde{t})$ of cases (a) BN1 (D=18), BN2 (D=22.16) and a uniform fuselage (D=18); (b) BN3 (D=14.64), BN4 (D=18) and a uniform fuselage (D=18). Solid and dashed lines show FE and Riera model results, respectively.

Figures 5(a) and (b) shows $f(\tilde{t})$ functions of cases EN1-4 and uniform fuselages, with eight times higher strength f_y than that of cases BN1-4.

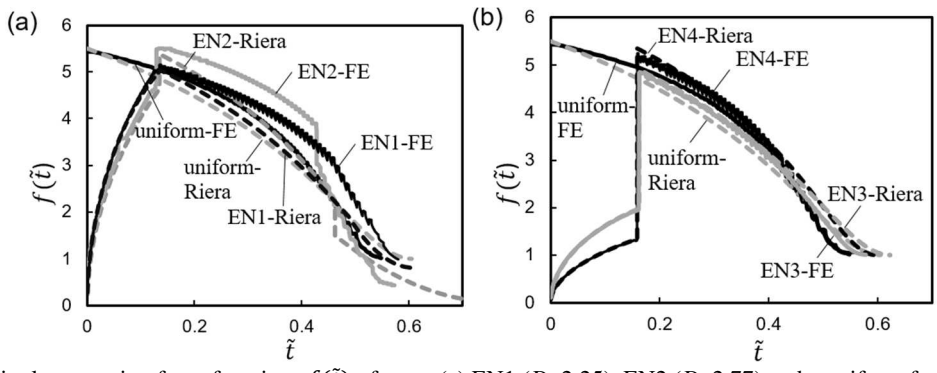

Fig. 5: Dimensionless reaction force functions $f(\tilde{t})$ of cases (a) EN1 (D=2.25), EN2 (D=2.77) and a uniform fuselage (D=2.25); (b) EN3 (D=1.83), EN4 (D=2.25) and a uniform fuselage (D=2.25). Solid and dashed lines show FE and Riera model results, respectively.

In case of cases EN1-4, due to the increased strength and crushing force, the missiles significantly decelerate during the impact, and consequently not the whole missiles crush during it. In cases EN1 and EN2, deceleration is more intense in the Riera model than in the FE model, therefore $f(\tilde{t})$ functions of the Riera model also decrease more intensely. Effect of strength cannot be neglected in cases EN1-4, in Eq. (1) the maximum relative value of $P(x)$ is 1, while the maximum value of f is 5.5. If Figs. 5(a) and (b) are compared, then effect of reduced strength is still less significant (case EN2 compared to case EN1) than effect of reduced density (case EN3 compared to case EN4). FE and Riera model result of cases EN3 and EN4 (see Fig. 5(b)) are closer to each other than FE and Riera model result of cases EN1 and EN2 (see Fig. 5(a)). It is advantageous because in case of real aircrafts the nose and tail parts are lighter and weaker than middle part of the fuselage, consequently case EN4 is the closest to real aircraft fuselage properties.
The relative difference between the FE and the Riera model results is calculated at each time instant as

$$\Delta f(\tilde{t}) = \frac{f_{\mathrm{FE}} - f_{\mathrm{R}}}{f_{\mathrm{R}}}, \tag{4}$$

where f_{R} and f_{FE} are the instantaneous dimensionless reaction force values obtained from the Riera and the FE model, respectively. Then absolute value of $\Delta f(\tilde{t})$ is averaged over the whole time span of the impact to obtain $\langle|\Delta f(\tilde{t})|\rangle$.
Figure 6 shows the temporal averages $\langle|\Delta f(\tilde{t})|\rangle$ of the relative difference Δf between the Riera and FE model results, as a function of the damage potential D. The represented cases include uniform missiles (with μ=const. and P=P_0=const.) and fuselages with nose and tail geometry and with density and strength ratio $\rho_{\mathrm{n}}/\rho = f_{\mathrm{yn}}/f$=0.25. Based on [5-6], in case of uniform missiles the damage potential D characterises the impact and the difference between the Riera and FE model results also depends on in.
We can see that $\langle\Delta f(\tilde{t})\rangle$—$D$ curves are similar in case of uniform missiles and fuselages with nose and tail: at high D values (D>10) the difference between the Riera and FE models is small, the impact is soft and both models are valid. As D decreases, the difference increases and has a local maximum around D=3-6. In this regime, in the Riera model, there is an intense deceleration during the impact, while deceleration is smaller or negligible in the FE model. If D is further decreased (D<2-2.5) then the collision in both models becomes a hard impact, and local effects become dominant, consequently neither the Riera nor the FE models are reliable in this regime.

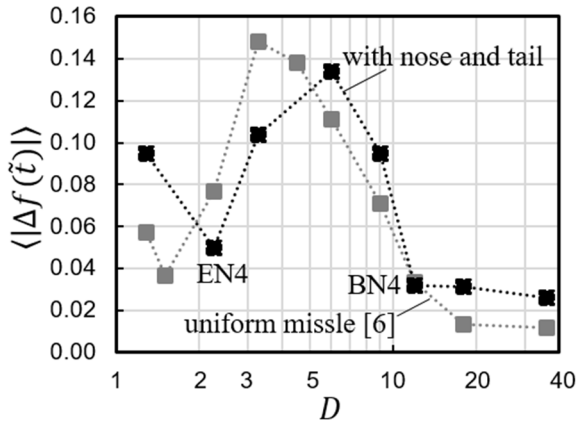

Fig. 6: Temporal average $\langle|\Delta f(\tilde{t})|\rangle$ of the absolute value of the relative difference (Eq.(4)) between instantaneous reaction force functions $f(\tilde{t})$ obtained from the Riera and FE models as a function of damage potential, in case of uniform missiles [6] and fuselages with nose and tail and with density and strength ratio $\rho_{\mathrm{n}}/\rho = f_{\mathrm{yn}}/f$=0.25

The effects of even more realistic aircraft geometry are also examined by adding wings and engines to the aircraft model. The geometry of the investigated aircrafts is close to the geometry of a Phantom F4 fighter applied in the full-size experiment by Sugano et al. [7]. In the FE and the Riera models, beside the fuselage, wings and engines also appear (see Fig. 2.). Vertical and horizontal tail wings are neglected, because their mass and crushing force is negligible compared to the other parts of the aircraft [7].The length and geometry of the fuselage are the same as in cases BN1 and EN1, the length and the outer diameter of the engines are 3.6 m and 0.3 m, respectively. As a simplification, the density and the strength of each part are kept constant in the FE model. The wall thicknesses of the parts are set to make mass distributions of the aircraft close to the distributions measured by Sugano et al. [7]. In the FE model, the wall thickness of the engines and wings are 0.16 m and 0.025 m, respectively, while finite element sizes in the longitudinal direction is 0.2 m in the wing and 0.15 m in the engine, while there is only one layer of elements along the thickness.
In our analyses, two different aircraft models are applied (see Table 2). Cases BT and ET have the same density, strength and velocity as cases BN1 and EN1, respectively (see Table 1). Table 2 also includes the total mass m_0, the maximum $P_{\max}$ and average value P_{av} (weighted by length) of the crushing force and the damage potentials $D(P_{\mathrm{av}})$. In the calculation of the crushing force and the damage potential, all parts of the aircrafts are included. Figure 7 shows the shape function of mass distribution and crushing force of cases BT and ET, together with shape functions of cases BN1, EN1, BN4 and EN4.

Table 2: Input data of cases BT and ET:

	body		*nose, tail, wing, engine*					
case	ρ	f_y	$\rho_{n,w}/\rho$	$f_{yn,yw}/f_y$	m_0	P_{max}	P_{av}	D (P_{av})
	(kg/m^3)	(10^6 Pa)	[-]	[-]	(10^3 kg)	(10^6 N)	(10^6 N)	
BT	8000	5	1	1	28.6	2.57	1.01	18
ET	8000	40			28.6	20.57	8.06	2.25

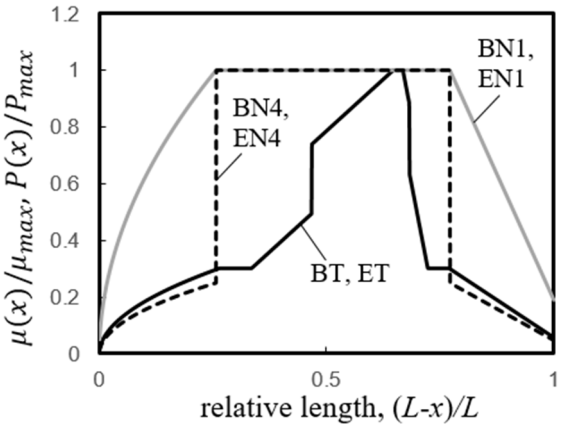

Fig. 7: Shape function of mass distribution and crushing force of cases BN1, EN1, BN4, EN4, BT, ET

Dimensionless reaction force—time functions $f(\tilde{t})$ of cases BT and ET are represented in Fig. 8. The shape of the curves follows the shape of the distributed mass and crushing force curves (Fig. 7), the crushing of the wings and engines cause a maximum reaction force around half of the total impact time. In case of ET aircraft, due to the high crushing force of the engines and the central segment of the fuselage, the velocity and consequently the reaction force intensely decrease at the last part of the impact. It is visible that the FE and Riera model results are close to each other in both cases, $\langle|\Delta f(\tilde{t})|\rangle$=0.046 and 0.067 for cases BT and ET, respectively. It is advantageous if we concern the applicability of the Riera and FE models in case of realistic aircrafts.

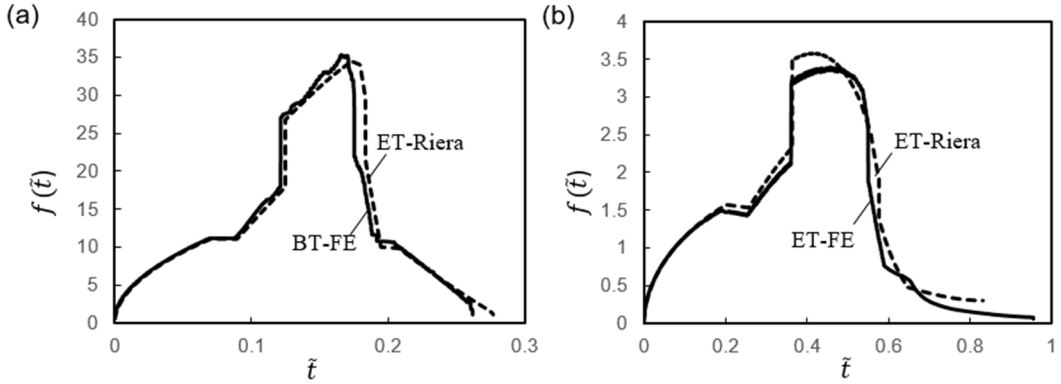

Fig. 8: Dimensionless reaction force functions $f(\tilde{t})$ of cases (a) BT (D=18); (b) ET (D=2.25). Solid and dashed lines show FE and Riera model results, respectively.

Conclusions

In our analysis the force acting on a rigid structure during soft aircraft impact is calculated by the widely used analytic Riera model [4] and by finite element models. The effect of realistic aircraft profiles is examined, therefore uniform aircraft fuselages (cylindrical missiles), aircraft fuselages with nose and tail, and simplified aircrafts with wings and engines are applied, and results are compared. One of our main findings is that the behaviour of the Riera and the FE models is closer to each other in case of more realistic aircraft profiles. This is advantageous if we consider the practical applicability of these models. We also found that a single parameter that characterises the impact in case of uniform fuselages both in the Riera and FE models [5-6] is also dominant in case of more realistic profiles. This parameter, the damage potential D, defined as the ratio of the initial kinetic energy of the missile to the work required to crush it, also influences dominantly the difference between the Riera and FE model results and also can characterise the impact. Similarly to uniform missiles [6], at high D values (D>10) the difference between the Riera and FE models is small, the impact is soft and both models are applicable. As D decreases, the difference increases and has a local maximum around D=3-6, in this regime, in the Riera model, there is an intense deceleration during the impact, while deceleration

is small or negligible in the FE model. If D further decreases ($D<2$-2.5) then the impact in both models becomes hard, and local effects become dominant, consequently, neither the Riera nor the FE models are reliable.

Acknowledgement

Lili Eszter Laczák is supported through the New National Excellence Program of the Ministry of Human Capacities.

References

[1] International Atomic Energy Agency (2003) IAEA Safety Standard Series External Events Excluding Earthquakes in the Design of Nuclear Power Plants, Safety Guide No. NS-G-1.5. IAEA, Vienna.
[2] U.S. Department of Energy (2006) DOE Standard, DOE-STD-3014-2006.Accident analysis for aircraft crash into hazardous facilities. DOE, Washington DC.
[3] Nuclear Energy Institute (2011) Methodology for performing aircraft impact assessments for new plant designs. NEI 07–13 [Revision 8P]. NEI, Washington DC.
[4] Riera, J.D. (1968) On the stress analysis of structures subjected to aircraft impact forces. *Nuclear Engineering and Design* **8**:415-426.
[5] Laczák, L.E., Károlyi Gy. (2017) On the impact of a rigid–plastic missile into rigid or elastic target. *International Journal of Non-Linear Mechanics* **91**:1-7.
[6] Laczák, L.E., Kollár L., Károlyi Gy. (2017) A dimensionless parameter to characterize the impact of a soft cylindrical missile into a robust target. Submitted for publication.
[7] Sugano, T., Tsubota H., Kasai Y., Koshika N., Orui S., von Riesemann W.A., Bickel D.C., Parks M.B. (1993) Full-scale aircraft impact test for evaluation of impact force. *Nuclear Engineering and Design* **140**:373-385.